

Structural disorder and silanol groups content in amorphous SiO₂

E. Vella* and R. Boscaino

Dipartimento di Scienze Fisiche ed Astronomiche, Università di Palermo, Via Archirafi 36, I-90123 Palermo, Italy

(Received 31 October 2008; published 13 February 2009)

We present a study on the features of the Urbach edge in amorphous silicon dioxide (*a*-SiO₂). The effects of temperature on the absorption edge in the range from 4 to 300 K were studied in both materials having negligible (*dry*, $<10^{17}$ cm⁻³) and significant (*wet*, $>10^{19}$ cm⁻³) silanol groups contents. Remarkable differences in the values and in the temperature dependence of the Urbach energy in the dry and wet samples were observed. These differences are interpreted as a consequence of a drastic reduction in the degree of disorder in wet materials, which turn out to be characterized by an electronic structure more similar to that of crystalline quartz. Furthermore, our results indicate that silanol groups affect the thermal component of disorder, modifying the vibrational modes of the network.

DOI: 10.1103/PhysRevB.79.085204

PACS number(s): 61.43.Er, 71.55.Jv, 78.40.Pg, 71.23.Cq

I. INTRODUCTION

Crystalline and amorphous semiconductors and insulators are characterized by exponential optical-absorption edges, generally referred to as *Urbach edges*.¹ Several experimental and theoretical studies evidence that disorder affects the features of the absorption edge both in crystalline and amorphous materials.^{2–10} In particular, thermal disorder smoothes the absorption edge in crystalline systems,^{1,3} whereas the absorption edge of amorphous materials is affected both by a thermal and a nonthermal component of disorder.^{2–4} The nonthermal (structural) disorder is peculiar of amorphous materials and originates from the intrinsic lack of long-range order and from point defects (e.g., dangling bonds and impurities). Structural disorder causes localized electronic states in the immediate neighborhood of the band edges, thus smearing out the absorption edge.^{1,11}

The analysis of the intrinsic absorption spectral region of amorphous silicon dioxide (*a*-SiO₂), from ~ 8 to ~ 9 eV, has recently received great attention because of the employment of this material in F₂ ($\lambda=157$ nm and $E=7.9$ eV) excimer lasers devices. The use of *a*-SiO₂ in this kind of applications requires an understanding of the effects of structural disorder on the optical properties. Most of the experimental works on this issue^{3,4,6,7,12} were carried out on dry silica, where the content of silanol groups is negligible, typically less than 10^{17} cm⁻³. The reason of this choice is that Si-OH groups are known to contribute to the optical absorption in the same spectral region [vacuum UV (vuv), $\lambda < 190$ nm, and $E > 6.5$ eV]^{9,13–22} and the overlap makes it difficult to isolate the tail of the intrinsic absorption. On the other hand, the study of the effects of structural disorder in wet materials is interesting because silanol groups are suspected to favor the relaxation of the network and to affect the structural disorder degree.^{9,23–25}

The structural disorder of the *a*-SiO₂ network can be described by means of another parameter: the fictive temperature (T_f). The *a*-SiO₂ matrix can, indeed, be represented as a frozen-in state whose structure corresponds to a supercooled liquid at a certain temperature. This temperature is the so-called fictive temperature. It is known that one of the most important topological modifications related with changes in

T_f is the average Si-O-Si bond angle: an increase in the fictive temperature is associated with a decrease in the mean Si-O-Si bond angle.²⁶

In this paper we present a study of the intrinsic absorption edge of both dry and wet *a*-SiO₂'s. The structural features (T_f) and the silanol groups concentrations of the examined materials were characterized via their infrared (IR) absorption spectra. In order to distinguish the thermal component of disorder from the nonthermal one, we analyzed the vuv spectra as a function of temperature in the range from 4 to 300 K. We observed that the modifications of the absorption edge induced by lowering temperature are different in dry and wet materials. We found, in particular, that the Urbach edge parameters of wet materials at low temperatures are comparable to those observed in α -quartz. This result is interpreted in terms of a drastic reduction in the degree of structural disorder in wet *a*-SiO₂.

II. OPTICAL-ABSORPTION EDGE OF AMORPHOUS SiO₂

The optical-absorption edge of amorphous SiO₂ can be represented by the exponential *Urbach law*,

$$\alpha(E) = \alpha_0 \exp\left(\frac{E - E_g}{E_u}\right), \quad (1)$$

where $\alpha(E)$ is the absorption coefficient, E_g is the optical energy gap, α_0 is a parameter characteristic of the material, and E_u is called the Urbach energy and depends on temperature. E_g and E_u , respectively, measure the position and the steepness of the absorption edge and control the transparency of the material in the vuv region. E_u can be used as an indicator of the disorder degree of the network, which, as mentioned before, is due to both thermal effects and to the frozen-in topological disorder. To take into account both contributions, the temperature dependence of the Urbach energy is usually described by the following equation:^{2,4}

$$E_u(T) = \frac{1}{\sigma_0} \left(E_T(T) + X \frac{\hbar \omega_0}{2} \right), \quad (2)$$

where

$$E_T(T) = \hbar\omega_0 \left(\frac{1}{2} + \frac{1}{\exp(\hbar\omega_0/k_B T) - 1} \right) = \frac{\hbar\omega_0}{2} \coth\left(\frac{\hbar\omega_0}{2k_B T}\right). \quad (3)$$

Equation (2) includes a temperature-related and a temperature-independent terms. The temperature-related term, $E_T(T)$, is the energy of thermal vibrations approximated by a single oscillation frequency ω_0 (Einstein model). The temperature-independent term is expressed for convenience as proportional to the zero-point vibrational energy $\hbar\omega_0/2$ through a dimensionless factor X representing the ratio between the static disorder contribution and the zero-point thermal contribution. Finally, in Eq. (2) σ_0 is a temperature-independent constant. In the Toyozawa theory^{27–29} σ_0 is inversely proportional to the exciton-phonon interaction strength.

According to Eqs. (2) and (3), as temperature decreases, the Urbach energy gets lower and the absorption edge steeper. These equations were used in literature⁴ to describe the temperature-induced changes in the absorption edge of dry *a*-SiO₂ and to allow us to distinguish the thermal from the nonthermal contribution to disorder. In the following we will use Eqs. (2) and (3) to represent the temperature dependence of the measured Urbach energy values in wet materials.

III. EXPERIMENTS

A. Experimental procedure and samples

We examined both dry and wet samples. A dry sample of Suprasil F300 [F300, type IV (Ref. 30)] was considered, while two types³⁰ of wet *a*-SiO₂ glasses were studied: a type III (synthetic wet) Suprasil 1 (S1) sample and a sol-gel (SG) sample. In the following we will refer to the different samples with the nicknames put in parentheses. The S1 and F300 materials were supplied by Heraeus Co.,³¹ while the SG sample was produced by Degussa Novara Technology by the SiVARA sol-gel process. It has to be noted that the F300 material has a chlorine concentration of $\sim 3.5 \times 10^{19} \text{ cm}^{-3}$ (~ 1000 ppm by weight) as declared by the producer.

The samples were $5 \times 5 \times 0.15 \text{ mm}^3$ in size and optically polished on the larger surfaces. Only the SG sample had a greater thickness ($\sim 0.3 \text{ mm}$). In our experimental setup the sample thickness, 0.15 mm, allows us to measure values of the vuv absorption coefficients as high as $\alpha(E) \sim 650 \text{ cm}^{-1}$; this condition sets the upper limit of the investigated spectral range up to $\sim 8.3 \text{ eV}$ ($\lambda \sim 149 \text{ nm}$). This range is wide enough to evidence the exponential region of the absorption edge and to measure E_u .

Vuv absorption spectra were obtained using an ACTON single-beam spectrophotometer (mod.SP150) working in N₂ flux (typically 80 l/min). To perform temperature-controlled absorption measurements in the temperature range from 4 to 300 K, the original sample chamber was home modified to host the optical cryostat (Optistat CF-V, produced by Oxford instruments) working in a continuous liquid Helium flow equipped with two MgF₂ windows. A two stage rotary/turbomolecular pump (Leybold Vacuum PT 50) is used to

achieve high vacuum in the cryostat by overnight pumping (base pressure $\sim 10^{-6}$ mbar). Thermal equilibrium within 1 K at the working temperature was achieved by an Oxford-ITC503 instrument, controlling the He flow. The spectrophotometer is equipped with a 30 W D₂ lamp and with two identical monochromators (1200 lines/mm, stray light $< 5 \times 10^{-4}$). The first monochromator selects the light going into the sample chamber, while the second filters the light coming out from it, and it is necessary in order to reduce stray light and possible luminescence emissions. These effects could, indeed, be particularly detrimental for the measurements in the spectral region we are interested in because the transmitted light is very low. Measurements were performed with a bandwidth [full width at half maximum (FWHM)] of 0.4 nm. For a reliable measurement of the Urbach edge experimental spectra were corrected for the photomultiplier dark current and surface reflections. The latter were estimated using literature data³² of the refractive index in *a*-SiO₂ at room temperature. The refractive index values at room temperature were used to correct the vuv measured spectra acquired at all the examined temperatures for it is known^{33,34} that the temperature-induced changes in the refractive index in the range of temperatures and of energies close to those we explored are within $\sim 0.003\%$, which is negligible for our purposes.

Optical densities lower than ~ 2.7 could be measured with an accuracy of ± 0.03 . We verified the reliability of the experimental setup and the analysis procedure by measuring the absorption edge in a sample of crystalline quartz at room temperature: the obtained value of E_u ($48 \pm 4 \text{ meV}$) is in fair agreement with literature data.³ The error on the estimate of the E_u values is within $\sim 10\%$.

The silanol groups concentration and the fictive temperature were determined from IR absorption spectra at room temperature. These were measured by a Bruker Vertex 70 Fourier transform IR single-beam absorption spectrometer equipped with a medium-IR light globar source. Spectra were acquired with a spectral resolution of 1 cm^{-1} . The errors on the determination of the position and the intensity of the IR bands of our interest are $\pm 0.05 \text{ cm}^{-1}$ and less than 1%, respectively.

B. Experimental results

In Fig. 1 the room-temperature IR absorption spectra of our samples in the range from 3400 to 3900 cm^{-1} are reported. As it is possible to see from Fig. 1, in the dry material F300, the band at $\sim 3670 \text{ cm}^{-1}$ is not detectable. To determine the Si-OH groups contents we measured the amplitude of the band at $\sim 3670 \text{ cm}^{-1}$, which is ascribed to the stretching vibrational mode of silanol groups in *a*-SiO₂.³⁵ We used the value $77.5 \text{ l mol}^{-1} \text{ cm}^{-1}$ for the molar extinction coefficient.³⁶

IR absorption spectra were used also to determine the fictive temperature of the samples. Figure 2 shows the IR absorption spectra measured on our samples in the range from 2140 to 2340 cm^{-1} . It is known³⁷ that the peak position of the band at $\sim 2260 \text{ cm}^{-1}$ is related to T_f via the following phenomenological equation:

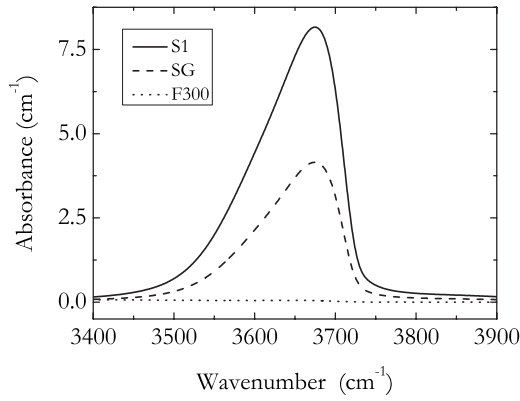


FIG. 1. Room-temperature IR absorption spectra of the three examined samples (S1, SG, and F300) in the region from 3400 to 3900 cm⁻¹.

$$\nu = 2228.64 + \frac{43\,809.21}{T_f}, \quad (4)$$

where ν is the frequency of the peak of the band. This band is the overtone of the IR structural absorption band at ~ 1120 cm⁻¹, which is attributed to the stretching vibrational mode of Si-O-Si linkages.³⁸ Using Eq. (4) and the position of the peak at ~ 2260 cm⁻¹ the fictive temperature of each examined sample was determined. In Table I the silanol groups contents and the fictive temperatures of our samples as estimated from the IR absorption spectra are reported.

Figure 3 shows the vuv absorption spectra of the S1 sample in the range of temperature from 4 to 300 K by steps of 30 K. At all the examined temperatures spectra can be described as composed of two different exponential regions. In Fig. 3 dashed lines evidence the two exponential profiles. As it was discussed in detail in a previous work,⁹ the low-energy exponential region is ascribed to the vuv absorption by Si-OH groups, while the high-energy exponential profile is the Urbach tail. The near-edge absorption spectra are significantly affected by temperature: with increasing temperature the amplitude of the silanol groups contribution in-

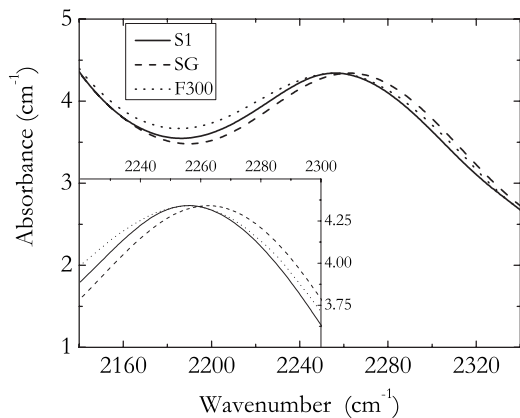


FIG. 2. Room-temperature IR absorption spectra of the three examined samples (S1, SG, and F300) in the region from 2140 to 2340 cm⁻¹. In the inset an enlargement of the peak of the bands is shown.

TABLE I. Si-OH concentration ($[\text{SiOH}]$) and fictive temperature (T_f) as experimentally estimated from the IR absorption spectra of the three examined samples.

Materials	$[\text{SiOH}]$ (cm ⁻³)	T_f (K)
S1	6.2×10^{19}	1570 ± 30
SG	3.2×10^{19}	1290 ± 20
F300	$< 10^{17}$	1610 ± 40

creases without changing its steepness, while the Urbach tail shifts toward lower energies and gets less steep. In the SG sample a similar behavior was observed.

In Fig. 4 the near-edge absorption spectra of the F300 sample in the range of temperatures from 4 to 300 K are reported. Unlike wet materials, in the studied range of temperatures the F300 vuv spectra can be represented as a single exponential, which is the Urbach absorption edge. Indeed, although Si-Cl and Si-OH groups are known to contribute to the absorption in the near-edge spectral region,^{9,39} this absorption cannot be ascribed to neither of these impurities. As far as Si-Cl groups are concerned, using the values of their absorption cross section estimated in literature³⁹ and the concentration of Si-Cl groups as declared by the producer ($\sim 3.5 \times 10^{19}$ cm⁻³), the contribution of Si-Cl groups to the absorption at 8 eV in the F300 material is ~ 10 cm⁻¹. Looking at the spectra in Fig. 4 it turns out that the observed absorption cannot be associated to these impurities. As to silanol groups, as evident from Fig. 1, their concentration in the F300 sample is negligible. Consequently in the vuv spectral region only the Urbach tail contribution to the absorption has to be observed.

In the dry sample the effect of lowering temperature consists in a shift of the Urbach tail toward higher energies, while the steepness of the spectra is only little affected by the decrease in temperature. We note that the explored range of values of the absorption coefficient does not allow us to evidence the crossing point of the lines obtained in a semilogarithmic scale as extrapolations of the Urbach tails at different temperatures. The crossing point is expected to be observed

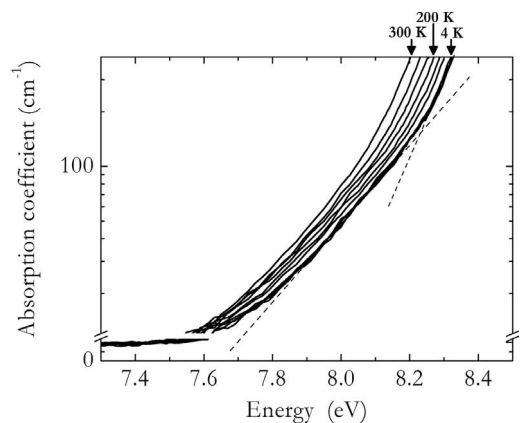


FIG. 3. Vuv absorption spectra of the S1 sample. Temperature ranges from 4 to 300 K by steps of 30 K. Dashed lines evidence the two exponential trends.

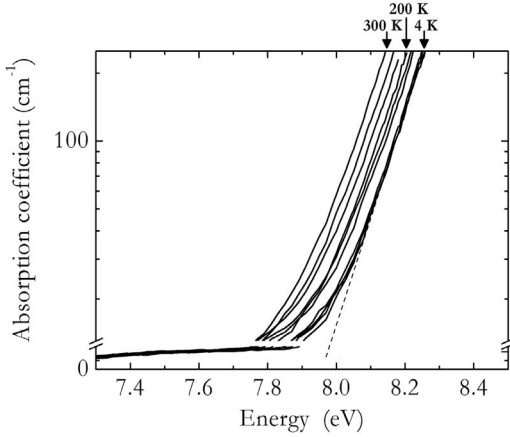


FIG. 4. Vuv absorption spectra of the F300 sample. Temperature ranges from 4 to 300 K by steps of 30 K. Dashed line evidences the exponential profile.

at a value of the absorption coefficient $\approx 10^{5.5} \text{ cm}^{-1}$,³ which is far beyond the range considered here.

Using a procedure discussed in detail in a previous work,⁹ we described the spectra of wet samples (S1 and SG) at all the examined temperatures as the sum of the following two functions:

$$Y = A_0 \exp\left(\frac{E - 8 \text{ eV}}{A_1}\right), \quad (5)$$

$$Y = Y_0 + 100 \exp\left(\frac{E - E_0}{E_u}\right). \quad (6)$$

Equation (5) represents the contribution of Si-OH groups to the vuv absorption, while Eq. (6) is the Urbach law rewritten in view of the fitting procedure. In Eq. (5) A_0 is the value of the absorption coefficient at 8 eV due to the silanol groups contribution only and A_1 is the inverse of the slope of the Si-OH exponential in a semilogarithmic scale. It was shown⁹ that at room temperature the A_0 value is linearly related to the silanol groups concentration as estimated from the IR spectra. In Eq. (6) E_0 is the energy value at which the contribution of the Urbach tail to the absorption coefficient is 100 cm^{-1} , E_u is the Urbach energy, and Y_0 is a parameter introduced to describe the profile of the absorption spectra in the range $< 7.5 \text{ eV}$. It is useful to compare Eq. (6) with Eq. (1). In Eq. (1) the Urbach law is expressed in terms of E_g , which is the optical energy gap. E_g depends on temperature and is generally estimated from the analysis of the absorption spectra in the so-called Tauc region, which is the spectral range just above the Urbach region.^{1,2,6} Since the measure of the absorption coefficient in the Urbach range only does not allow to define the pre-exponential factor α_g independently from the E_g value, we chose to express the Urbach law as a function of the E_0 parameter whose only meaning is that of the value of energy corresponding to an absorption coefficient of 100 cm^{-1} . However, E_0 can be used to estimate the changes in the transparency range as a function of temperature. The use of Eqs. (5) and (6) allows distinguishing the silanol groups contribution from the intrinsic one and reli-

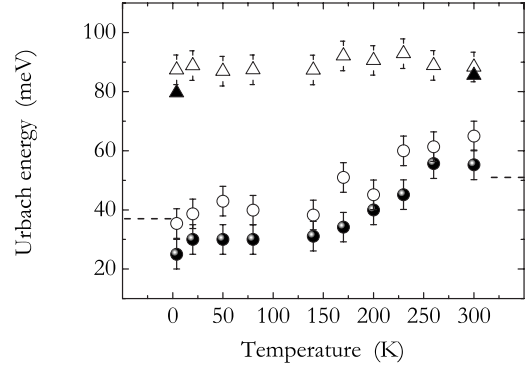


FIG. 5. Plot of the Urbach energy values as a function of temperature measured in: the S1 sample (empty circles), the SG sample (filled circles), and the F300 sample (empty triangles). The values of the Urbach energy observed in a dry material at 4 and 300 K as reported in Ref. 4 are shown for comparison (filled triangles). The dashed lines on the low- and high-temperature sides of the graph, respectively, show the Urbach energy values measured in α -quartz at 4 and 300 K as reported in Ref. 3.

ably determining the values of the Urbach energy in wet materials. The vuv spectra of the F300 sample were described, instead, using Eq. (6) only, for the sole Urbach tail is observed.

In Fig. 5 the values of the Urbach energy as determined from the fits of the vuv spectra are reported as a function of temperature. The E_u values of the dry F300 sample are not significantly affected by temperature in the whole range from 4 to 300 K and remain approximately constant around a value of $\sim 90 \text{ meV}$, which is appreciably higher than the Urbach energy measured in both wet samples at any of the examined temperatures. On the contrary the E_u values measured in wet materials show a strong dependence on temperature. As it is shown in Fig. 5, in both S1 and SG samples E_u does not vary up to a temperature of $\sim 100 \text{ K}$ and then it increases for higher temperatures. The fits of the vuv spectra allowed us to determine the E_0 values and thus to quantify the variations in the transparency range. In Table II the E_0 values at 4 and 300 K as determined from the fits of the vuv spectra of all examined samples are reported.

Finally, the Urbach energies values of the S1 and SG samples as a function of temperature were fitted using Eq. (2). In Fig. 6 the E_u values and the fitted curve for the SG sample are shown as an example. In Table III the values of the parameters $\hbar\omega_0$, σ_0 , and X [see Eq. (2)] as estimated from the fits of the Urbach energy values as a function of temperature in the S1 and SG samples are reported.

TABLE II. E_0 [see Eq. (6)] values at 4 and 300 K as determined from the fits of the vuv spectra of the three examined samples. The errors on the E_0 values are 0.05 eV.

Materials	$E_0(T=4 \text{ K})$ (eV)	$E_0(T=300 \text{ K})$ (eV)
S1	8.32	8.16
SG	8.34	8.19
F300	8.18	8.06

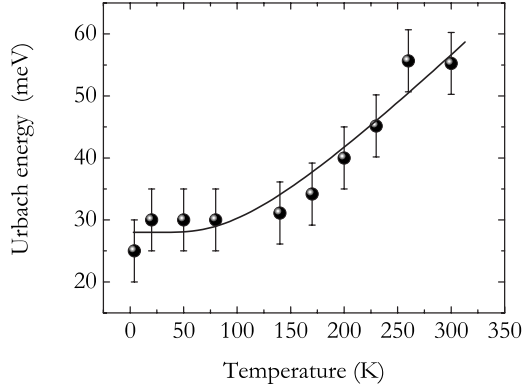


FIG. 6. Urbach energy values measured in the SG sample. The line was obtained by fitting the experimental data using Eq. (2) together with Eq. (3).

IV. DISCUSSION AND CONCLUSIONS

In the previous section we reported our experimental results on the temperature dependence of the intrinsic absorption tail in wet and dry α -SiO₂'s. In the present section we compare these two types of materials and speculate on the possible role of Si-OH groups.

First we note that the examination of the absorption edge in wet materials was possible, thanks to our procedure of analysis of vuv spectra, aimed at isolating the silanol groups contribution from the intrinsic one [Eqs. (6) and (5)] and yielding a reliable evaluation of the Urbach energy also in this type of material. The E_u values in wet α -SiO₂ were not reported previously.

According to our results, the temperature dependence of E_u in wet materials is essentially the same in the two silica types considered here (a type III and a sol-gel), in spite of the huge difference of the manufacture procedure and of the Si-OH groups content. This circumstance suggests that the measured temperature dependence of E_u manifests an intrinsic feature of the absorption tail, as conditioned by the presence of Si-OH groups.

As regard to dry materials, our results on the temperature dependence of the Urbach energy values are consistent with literature data. In particular Saito *et al.*⁴ investigated the temperature range from 4 to 1900 K and used the T dependence of E_u to infer the values of the $\hbar\omega_0$, σ_0 , and X parameters. Our outcomes are coherent with the just mentioned data although exploring only the low-temperature range. The com-

TABLE III. Fitting parameters of the function describing the Urbach energy temperature dependence [see Eqs. (2) and (3)] in the S1 and SG samples: $\hbar\omega_0$, σ_0 , and X . The values of the fitting parameters as estimated in Ref. 4 for a dry material are presented for comparison.

Materials	X	$\hbar\omega_0$ (eV)	σ_0
S1	0.17 ± 0.05	0.032 ± 0.005	0.48 ± 0.05
SG	0.15 ± 0.05	0.026 ± 0.005	0.54 ± 0.05
Dry α -SiO ₂ ^a	0.33 ± 0.03	0.079 ± 0.008	0.66 ± 0.05

^aReference 4.

parison with data reported in Ref. 4 is fairly satisfying: this can be seen in Fig. 5, where the Urbach energy values as reported in Ref. 4 at 4 and 300 K are also shown (filled triangles) for the sake of comparison with our results.

Wet and dry materials strongly differ with respect to both the structural and thermal contributions to disorder. The low-temperatures limit of the Urbach energy actually evidences the structural contribution to disorder. The E_u values observed at 4 K in wet samples are drastically lower than those observed in the dry one. Moreover, in Fig. 5 the values of the Urbach energy measured on a sample of α -quartz at 4 and 300 K as reported in Ref. 3 are shown for comparison. As it is possible to see, $E_u(4\text{ K})$ in wet samples (35 and 30 meV in the S1 and SG samples, respectively) is comparable with the Urbach energy measured at the same temperature in a sample of crystalline SiO₂ (~ 37 meV).³ This outcome is an evidence of a severe reduction in structural disorder in wet α -SiO₂ with respect to dry ones. This can be considered as a consequence of the fact that silanol groups ($>10^{19}$ cm⁻³) limit the stabilization of the electronic localized states related to structural disorder, responsible for the absorption in the Urbach region. This effect cannot be directly ascribed to the capability of silanol groups of disrupting the SiO₄ tetrahedral network. Indeed, although it is known that Si-Cl groups dissociate the α -SiO₂ network as Si-OH groups do and enhance the structural relaxation as well,⁴⁰ in the F300 sample, whose Si-Cl groups content is significant ($\sim 3.5 \times 10^{19}$ cm⁻³), the low-temperatures limit of the Urbach energy is much higher (~ 90 meV). Our results suggest that silanol groups limit the stabilization of electronic localized states not only by favoring the structural relaxation. Thus, it turns out that a noticeable concentration of silanol groups, instead of increasing the frozen-in disorder, makes the α -SiO₂ electronic structure more similar to that of crystalline quartz and that this effect is not directly related to the fact that silanol groups are network modifier impurities because other network modifiers, such as Si-Cl groups, have not a similar effect.

Wet materials differ from the dry ones also as regard to the thermal component of disorder. This fact is actually proved by the values of $\hbar\omega_0$. The differences observed in the temperature dependence of E_u originates from a value of $\hbar\omega_0$ in wet materials lower than in the dry ones (see Table III). This means that silanol groups affect the vibrational properties of the amorphous network, in particular favoring softer vibrational modes.

As for the σ_0 values, we estimated that they are smaller in wet materials (see Table III). As this parameter is inversely proportional to the exciton-phonon coupling strength,²⁷⁻²⁹ our results show that the interaction between phonons and excitons is stronger in wet materials. In order to interpret this datum, it is useful to mention that the exciton-phonon interaction was proposed⁴¹ being stronger for excitons localized on impurities. In this context, it may be guessed that the lower values of σ_0 observed in wet materials are a consequence of the formation of excitons localized on silanol groups.

We did not find a direct influence of the structural component of disorder, as probed by the low-temperature Urbach energy values, on the fictive temperature. Indeed, if we compare the T_f values (see Table I), we notice that the S1 and

F300 samples show comparable fictive temperature values but appreciably different low-temperature E_u values. This outcome suggests that the reduction in structural disorder is not related to a variation in the value of the Si-O-Si bond angle. It may be argued, instead, that it influences the width of the bond-angle distribution, in particular favoring a narrower distribution. The Si-O-Si bond angle distribution can be tentatively probed by the width of the ~ 2260 cm^{-1} band. Although spectra reported in Fig. 2 suggest that this band actually has a greater width in the F300 dry sample, this issue requires a more careful study because of the difficulties related with the determination of the width of the ~ 2260 cm^{-1} band due to its closeness to other absorption contributions.

The blueshift of the transparency range is comparable in the two wet samples (0.16 and 0.15 eV for the S1 and SG samples, respectively), and it does not differ significantly from that observed in the dry material (0.12 eV for the F300 sample). Although the E_0 parameter gives only indirect information about the optical gap, this circumstance suggests that the temperature dependence of the optical gap is comparable in wet and dry α -SiO₂'s.

As a final remark, we mentioned that the silanol groups contribution to the absorption in the vuv spectral range de-

creases with decreasing temperature in the range from 300 to 4 K. With regards to this aspect, it is important to remark that silanol groups are known to exist in α -SiO₂ in several bond configurations.^{15,36,42-44} Our results do not address the question concerning the role of the different subspecies on the vuv absorption. On the other hand, they suggest that the concentration of the Si-OH subspecies responsible of the near-edge absorption is affected by temperature and that a temperature-induced conversion process from one subspecies to another is effective. Work is in progress in order to clarify this issue.

ACKNOWLEDGMENTS

We thank Degussa Novara Technology (Evonik Industries GmbH) for carefully preparing the sol-gel sample. Technical assistance by G. Tricomi, G. Napoli, and G. Lapis is acknowledged. We are grateful to all the members of the LAMP group (Ref. 45) for continuous stimulating discussions. We wish in particular to thank Michele D'Amico and Fabrizio Messina for their generous cooperation to devise and carry out cryogenic measurements.

*eleonora.vella@fisica.unipa.it

- ¹J. Tauc, *Amorphous and Liquid Semiconductors* (Plenum, London, 1974).
- ²G. D. Cody, T. Tiedje, B. Abeles, B. Brooks, and Y. Goldstein, *Phys. Rev. Lett.* **47**, 1480 (1981).
- ³I. T. Godmanis, A. N. Trukhin, and K. Hubner, *Phys. Status Solidi B* **116**, 279 (1983).
- ⁴K. Saito and A. J. Ikushima, *Phys. Rev. B* **62**, 8584 (2000).
- ⁵H. Hosono, Y. Ikuta, T. Kinoshita, K. Kajihara, and M. Hirano, *Phys. Rev. Lett.* **87**, 175501 (2001).
- ⁶K. Saito and A. J. Ikushima, *J. Appl. Phys.* **91**, 4886 (2002).
- ⁷L. Skuja, K. Kajihara, Y. Ikuta, M. Hirano, and H. Hosono, *J. Non-Cryst. Solids* **345-346**, 328 (2004).
- ⁸E. Vella, R. Boscaino, G. Navarra, and B. Boizot, *J. Non-Cryst. Solids* **353**, 559 (2007).
- ⁹E. Vella, R. Boscaino, and G. Navarra, *Phys. Rev. B* **77**, 165203 (2008).
- ¹⁰T. Tamura, S. Ishibashi, S. Tanaka, M. Kohyama, and M.-H. Lee, *Phys. Rev. B* **77**, 085207 (2008).
- ¹¹S. R. Elliott, *Physics of Amorphous Materials* (Longmans, Harlow, England, 1984).
- ¹²J. Platt, *Solid State Commun.* **136**, 201 (2005).
- ¹³K. Awazu and H. Kawazoe, *J. Non-Cryst. Solids* **179**, 214 (1994).
- ¹⁴Y. Ikuta, S. Kikugawa, A. Masui, A. Shimodaira, S. Yoshizawa, and M. Hirano, *Proc. SPIE* **3676**, 857 (1999).
- ¹⁵Y. Morimoto, S. Nozawa, and H. Hosono, *Phys. Rev. B* **59**, 4066 (1999).
- ¹⁶H. Hosono and Y. Ikuta, *Nucl. Instrum. Methods Phys. Res. B* **166-167**, 691 (2000).
- ¹⁷K. Kajihara, Y. Ikuta, M. Hirano, T. Ichimura, and H. Hosono, *J. Chem. Phys.* **115**, 9473 (2001).

- ¹⁸K. Kajihara, L. Skuja, M. Hirano, and H. Hosono, *Appl. Phys. Lett.* **79**, 1757 (2001).
- ¹⁹H. Hosono, K. Kajihara, T. Suzuki, Y. Ikuta, L. Skuja, and M. Hirano, *Solid State Commun.* **122**, 117 (2002).
- ²⁰N. Kuzuu, H. Horikoshi, T. Nishimura, and Y. Kokubo, *J. Appl. Phys.* **93**, 9062 (2003).
- ²¹K. Kajihara, M. Hirano, L. Skuja, and H. Hosono, *Phys. Rev. B* **72**, 214112 (2005).
- ²²K. Kajihara, M. Hirano, L. Skuja, and H. Hosono, *J. Non-Cryst. Solids* **352**, 2307 (2006).
- ²³U. Haken, O. Humbach, S. Ortner, and H. Fabian, *J. Non-Cryst. Solids* **265**, 9 (2000).
- ²⁴D. Shin and M. Tomozawa, *J. Non-Cryst. Solids* **203**, 262 (1996).
- ²⁵K. Saito, H. Kakiuchida, and A. J. Ikushima, *J. Appl. Phys.* **84**, 3107 (1998).
- ²⁶A. E. Geissberger and F. L. Galeener, *Phys. Rev. B* **28**, 3266 (1983).
- ²⁷Y. Toyozawa, *Prog. Theor. Phys.* **22**, 455 (1959).
- ²⁸H. Sumi and Y. Toyozawa, *J. Phys. Soc. Jpn.* **51**, 342 (1971).
- ²⁹M. Schreiber and Y. Toyozawa, *J. Phys. Soc. Jpn.* **51**, 1544 (1982).
- ³⁰R. Bruckner, *J. Non-Cryst. Solids* **5**, 123 (1970).
- ³¹Heraeus Quartzglas, Germany, catalog POL-0/102/E.
- ³²H. R. Philipp, *J. Phys. Chem. Solids* **32**, 1935 (1971).
- ³³J. Matsuoka, N. Kitamura, S. Fujinaga, and T. Kitaoka, *J. Non-Cryst. Solids* **135**, 86 (1991).
- ³⁴D. Leviton and B. Frey, *Proc. SPIE* **6273**, 62732K (2006).
- ³⁵J. E. Shelby, P. L. Mattern, and D. K. Ottesen, *J. Appl. Phys.* **50**, 5533 (1979).
- ³⁶K. M. Davis, A. Agarwal, M. Tomozawa, and K. Hirao, *J. Non-Cryst. Solids* **203**, 27 (1996).

- ³⁷A. Agarwal, K. M. Davis, and M. Tomozawa, *J. Non-Cryst. Solids* **191**, 185 (1995).
- ³⁸F. L. Galeener, *Phys. Rev. B* **19**, 4292 (1979).
- ³⁹K. Awazu, H. Kawazoe, K. Muta, T. Ibuki, K. Tabayashi, and K. Shobatake, *J. Appl. Phys.* **69**, 1849 (1991).
- ⁴⁰A. Koike and M. Tomozawa, *J. Non-Cryst. Solids* **353**, 2938 (2007).
- ⁴¹T. Sawai, *Suppl. Prog. Theor. Phys.* **53**, 222 (1973).
- ⁴²G. E. Walrafen and S. R. Samanta, *J. Chem. Phys.* **69**, 493 (1978).
- ⁴³V. G. Plotnichenko, V. O. Sokolov, and E. M. Dianov, *J. Non-Cryst. Solids* **261**, 186 (2000).
- ⁴⁴L. Nuccio, S. Agnello, and R. Boscaino, *Appl. Phys. Lett.* **93**, 151906 (2008).
- ⁴⁵<http://www.fisica.unipa.it/amorphous>